

STRUCTURE PECULIARITIES OF NANOCRYSTALLINE SOLID SOLUTIONS IN GdAlO_3 — GdFeO_3 SYSTEM

E. A. Tugova^{1,2}, V. V. Gusarov^{1,2}

¹Ioffe Physical Technical Institute of RAS, Saint Petersburg, Russia

²Saint Petersburg State Institute of Technology, Russia

katugova@inbox.ru; victor.v.gusarov@gmail.com

PACS 61.46.-w

Nanoparticles of solid solutions in GdAlO_3 — GdFeO_3 system have been synthesized. Plots of crystalline sizes for $\text{GdAl}_{1-x}\text{Fe}_x\text{O}_3$ series versus GdFeO_3 composition have been constructed. The sizes of solid solution nanoparticles were shown to decrease in comparison to the sizes of nanocrystalline individual compounds. The observed regularities allowed us to assume the formation of nanocrystalline $\text{GdAl}_{1-x}\text{Fe}_x\text{O}_3$ series with core-shell morphology.

Keywords: nanostructures, solid solutions, precipitation technique, non-autonomous phases, core-shell nanoparticles.

1. Introduction

Perovskite-type compounds possess unique electrical, magnetic, thermal properties [1–6]. Thus, the research of perovskite-like compounds and solid solutions based on it formation processes, as well as phase equilibria in systems, composing mentioned phases are of great interest [7–10]. Phase relations in pseudo-binary LnAlO_3 — LnFeO_3 section have been investigated in single works [11, 12] and basically were made for one LaAlO_3 — LaFeO_3 system. According to the presented data the solubility limits of LaAlO_3 and LaFeO_3 at 1200 °C were set to be $0 \leq x \leq 0.40$ for the $\text{LaFe}_{1-x}\text{Al}_x\text{O}_3$ series and $0 \leq y \leq 0.15$ for $\text{LaFe}_y\text{Al}_{1-y}\text{O}_3$ solid solutions [11]. Kuščer et al indicated the formation of continuous $\text{LaFe}_{1-x}\text{Al}_x\text{O}_3$ ($0 \leq x \leq 1$) series at 1300 °C [12]. Previously, samples were prepared by solid-phase chemical reactions using different starting components: hydroxides and oxides [11, 12].

It is of great interest to synthesize solid solutions based on nanoscaled perovskite-like oxides by “soft” chemistry methods [13–16]. The unusual effects observed during nanocrystalline solid solutions formation were fixed [17–19]. The mentioned effects were attributed to a number of factors, including the increase of component’s relative solubility in its nanosized state in comparison with macroparticles, the formation of nanoparticles with core-shell morphology and the decreasing of solid solutions nanoparticles sizes in comparison to those of nanocrystalline individual compounds.

These reasons demonstrate the importance of systematic investigations into the peculiarities of nanocrystalline solid solutions, and as a result, structural research with particular interest in the study of nanocrystallite formation in the GdAlO_3 — GdFeO_3 system was carried out.

2. Experimental

2.1. Synthesis procedure

$GdAl_{1-x}Fe_xO_3$ ($0 \leq x \leq 1$) series were prepared by precipitation from aqueous solutions of stoichiometric amounts of 1M $Gd(NO_3)_3 \cdot 5H_2O$, $Fe(NO_3)_3 \cdot 9H_2O$ and $Al(NO_3)_3 \cdot 9H_2O$. Aqueous 10 wt.% NH_4OH was used as the coagulating medium. To this NH_4OH solution aqueous solutions of gadolinium, iron and aluminum nitrates were added in a dropwise manner by adjusting the pH to 8–9. The co-precipitated mixtures were filtered immediately after preparation to remove traces of NO_3^- ions and were then dried at room temperature in air. The initial precipitates were subsequently pressed and calcined in air at 600–1300 °C for 3 h.

2.2. Characterization of prepared nanocrystals

The purity and crystallization of $GdAl_{1-x}Fe_xO_3$ samples were characterized by powder X-ray diffraction (XRD) using a Shimadzu XRD-7000 with monochromatic CuK_α radiation ($\lambda = 154.178$ pm). $\alpha-Al_2O_3$ was used as internal standard. Crystallite sizes of the obtained powders were calculated by the X-ray line broadening technique based on Scherer's formula.

3. Results and discussion

Fig.1 shows the X-ray powder diffraction (XRD) data of the initial mixture corresponding to stoichiometry of $GdAlO_3$, heat treated at 600 – 1300 °C for 3 h in air. The results of X-ray analysis of $GdAlO_3$ formation presented in Fig. 1 demonstrate the amorphous state of the initial mixture remains until 1000 °C. Crystallization of the $GdAlO_3$ phase is fixed at 1000 °C (Fig. 1). The latter is 300 °C higher than the temperature at which nanocrystalline $GdFeO_3$ is produced [20]. Thus, the investigation of the formation processes for $GdAl_{1-x}Fe_xO_3$ ($0 < x < 1$) solid solutions in $GdAlO_3 - GdFeO_3$ system was carried out at 1000–1300 °C. The ratio of components in $GdAlO_3 - GdFeO_3$ system was varied in 20 mol. % increments.

The mean size of coherent scattering regions of $GdAlO_3$ and $GdFeO_3$ individual perovskite-like compounds were approximately 60 nm.

The XRD patterns of initial mixtures corresponding to a stoichiometry of $GdAl_{1-x}Fe_xO_3$ ($0 < x < 1$) series which were heated at 1100 °C are presented in Fig. 2 as an illustration of the processing stages of target solid solutions research.

Fig. 3. shows the relationship between the mean size of coherent scattering regions and interstitial areas for peak with (111) index determined from X-ray data of the $GdAl_{1-x}Fe_xO_3$ series under 1000, 1100 and 1300 °C versus $GdFeO_3$ content.

The obtained data showed that the crystallite size of $GdAlO_3$ decreased at concentrations ranging from $0.2 < x < 0.5$ (Fig. 3), with the highest $GdFeO_3$ content giving the smallest values of 30–40 nm. These relationships are in agreement with data for interstitial areas (d/n) for the $GdAl_{1-x}Fe_xO_3$ series, for which the observed deviation of plotted d/n values from linearity were typical for solid solutions. These data can be connected with the formation of $GdAl_{1-x}Fe_xO_3$ nanoparticles with core-shell structure type which is in agreement with previous literature [18–19].

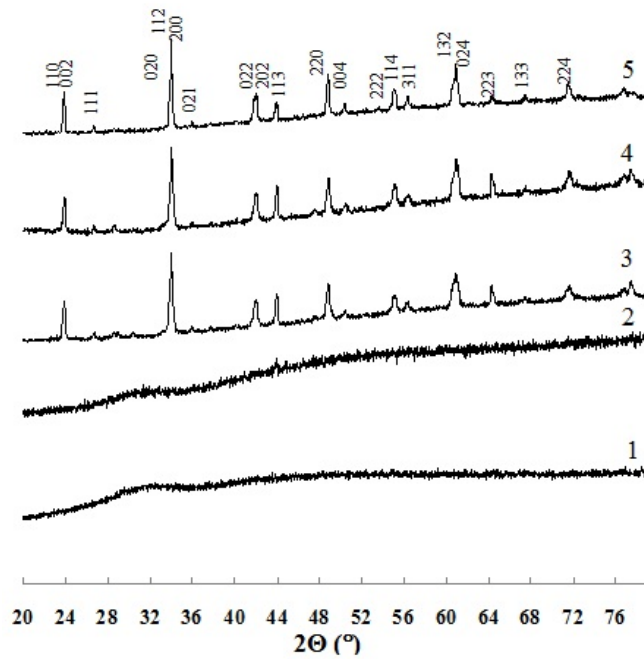


Fig. 1. X-Ray diffraction patterns of initial mixtures corresponding to stoichiometry of GdAlO_3 after sintering in air at °C: 1. 600; 2. 800; 3. 1000; 4. 1100; 5. 1300 °C for 3 h

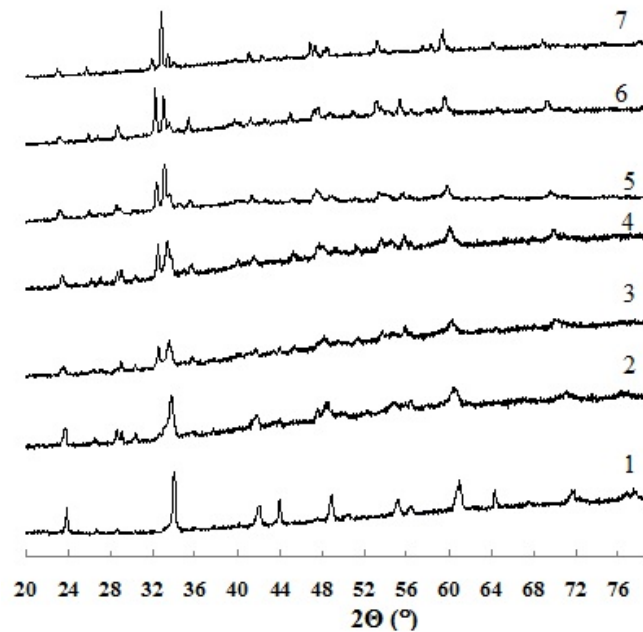


Fig. 2. X-Ray diffraction patterns, describing processes of $\text{GdAl}_{1-x}\text{Fe}_x\text{O}_3$ series formation for x : 1) 0; 2) 0.2; 3) 0.4; 4) 0.5; 5) 0.6; 6) 0.8; 7) 1 from initial mixtures heat treated at 1100 °C for 3 h

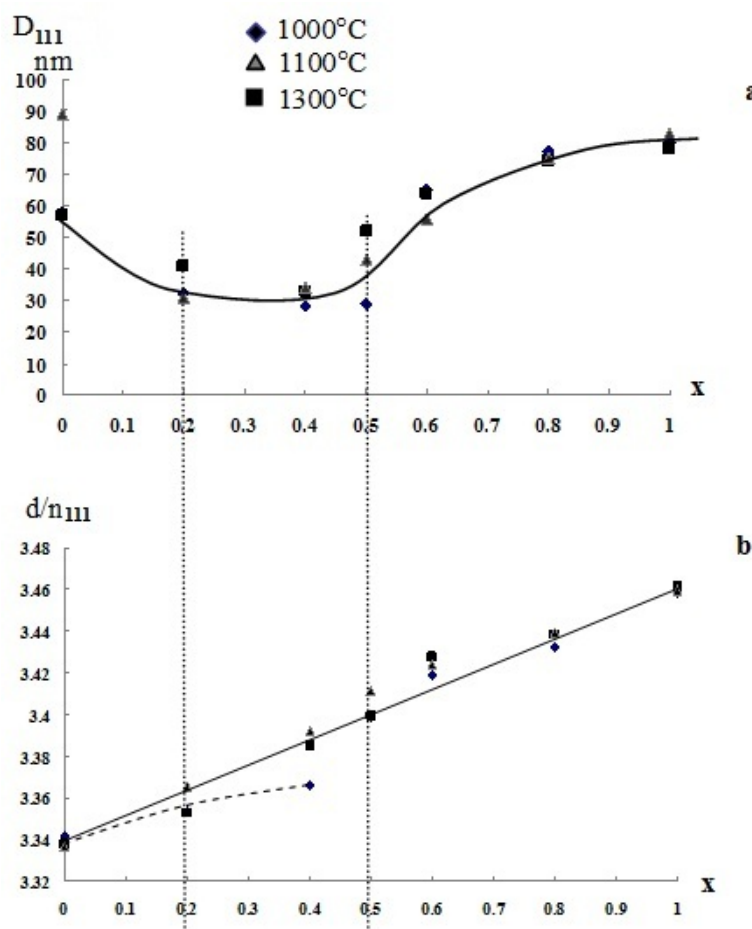


Fig. 3. a) The mean size of coherent scattering regions (D) and b) d/n for $GdAl_{1-x}Fe_xO_3$ series as a function of $GdFeO_3$ content (x)

4. Conclusion

These results showed that the formation of $GdAl_{1-x}Fe_xO_3$ continuous series in the $GdAlO_3-GdFeO_3$ system were observed at 1100-1300 °C. $GdAl_{1-x}Fe_xO_3$ nanoparticles ranging from 30–40 nm size were obviously attributed to the core-shell morphology.

Acknowledgments

This work was financially supported by the Russian Foundation for Basic Research, project No 13-03-00888.

References

- [1] Stølen S., Grønvold F., Brinks H. Heat capacity and thermodynamic properties of $LaFeO_3$ and $LaCoO_3$ from $T = 13$ K to $T=1000$ K, *J. Chem. Thermodynamics*, **30**, P. 365–377 (1998).
- [2] Zhang Yu., Yang J., Xu J., Gao Q., Hong Zh. Controllable synthesis of hexagonal and orthorhombic $YFeO_3$ and their visible-light photocatalytic activities. *Materials Letters*, **81**, P. 1–4 (2012).
- [3] Zong Ya., Fujita K., Akamatsu H., Murai Sh., Katsuhisa Tanaka K. Antiferromagnetism of perovskite $EuZrO_3$. *Journal of Solid State Chemistry*, **183**, P. 168–172 (2010).
- [4] Goto T., Kimura T., Lawes G., Ramirez A.P., Tokura Y. Ferroelectricity and giant magnetocapacitance in perovskite rare-earth manganites. *Physical review letters*, **92**, P. 257201 (2004).

- [5] Bondar' I. A., Shirvinskaya A. K., Popova V. F., Mochalov I. V., Ivanov, A. O., Thermal Stability of Orthoaluminates of Rare-Earth Elements of the Yttrium Subgroup. *Dokl. Akad. Nauk SSSR*, **246**(5), P. 1132–1136 (1979).
- [6] Petrosyan A. G., Popova V. F., Gusarov V. V., Shirinyan G. O., Pedrini C., Lecoq P. The $\text{Lu}_2\text{O}_3 - \text{Al}_2\text{O}_3$ system: relationships for equilibrium-phase and supercooled states. *J. Crystal Growth*, **293**, P. 74–77 (2006).
- [7] Tsipis E. V., Kharton V. V., Waerenborgh J. C., Rojas D. P., Naumovich E. N., Frade J. R. Redox behavior of acceptor-doped $\text{La}(\text{Al},\text{Fe})\text{O}_{3-\delta}$. *Journal of Alloys and Compounds*, **413**, P. 244–250 (2006).
- [8] Sagdahl L. T., Einarsrud M. A., Grande T. Sintering behaviour of $\text{La}_{1-x}\text{Sr}_x\text{FeO}_{3-\delta}$ mixed conductors. *J. Eur. Ceram. Soc.*, **26**, P. 3665–3673 (2006).
- [9] Ning L., Guoqing Ya., Guang Z., Huanyin G.. Effect of Dy doping on magnetism of $\text{La}_{0.7}\text{Sr}_{0.3}\text{CoO}_3$ system. *Rare Metals*, **31**(2), P. 135–139 (2012).
- [10] Savinskaya O. A., Nemudry A. P., Lyakhov N. Z. Synthesis and Properties of $\text{SrFe}_{1-x}\text{M}_x\text{O}_{3-z}$ (M=Mo, W) Perovskites. *Inorg. Mater*, **43**(12), P. 1350–1360 (2007).
- [11] Hrovat M., Holc J., Kuščer D., Bernik S. Preliminary data on subsolidus phase equilibria in the $\text{La}_2\text{O}_3-\text{Al}_2\text{O}_3-\text{Mn}_2\text{O}_3$ and $\text{La}_2\text{O}_3-\text{Al}_2\text{O}_3-\text{Fe}_2\text{O}_3$ systems. *J. Mater.Sci. Lett.* **14**(4). P. 265–267 (1995).
- [12] Kuščer D., Hanzžel D., Holc J., Marko Hrovat M., Kolar D. Defect Structure and Electrical Properties of $\text{La}_{1-y}\text{Sr}_y\text{Fe}_{1-x}\text{Al}_x\text{O}_{3-\delta}$. *J. Am. Ceram. Soc.*, **84**(5), P. 1148–1154 (2001).
- [13] Shivakumara C. Low temperature synthesis and characterization of rare earth orthoferrites LnFeO_3 (Ln=La, Pr and Nd) from molten NaOH flux. *Solid State Communications*, **139**, P. 165–169 (2006).
- [14] Popa M., Calderon Moreno J. M., Lanthanum ferrite ferromagnetic nanocrystallites by a polymeric precursor route. *Journal of Alloys and Compounds*, **509**, P. 4108–4116 (2011).
- [15] Cizauskaite S., Reichlova V., Nenartaviciene G., Beganskiene A., Pinkas J., Kareiva A. Sol-gel preparation and characterization of gadolinium aluminate. *Materials Chemistry and Physics*, **102**, P. 105–110 (2007).
- [16] Andrés-Vergés M., Morales M. del P., Veintemillas-Verdaguer S., Palomares F. Ja., Serna C.J., Core/shell magnetite/bismuth oxide nanocrystals with tunable size, colloidal and magnetic properties, *Chem. Mater.*, **24**, P. 319–324 (2012).
- [17] Melekhin V.G., Kolobkova E. V., Lipovskii A. A., Petrikov V. D., Almjasheva O. V. Formation of Nanostructures of the Core–Shell Type upon Diffusion Phase Decomposition of Fluorophosphate Glasses. *Glass Physics and Chemistry*, **33**(6), P. 569–575 (2007).
- [18] Tomkovich M. V., Andrievskaya E. R., Gusarov V. V. Formation under hydrothermal conditions and structural features of nanoparticles based on the system $\text{ZrO}_2-\text{Gd}_2\text{O}_3$. *Nanosystems: physics, chemistry, mathematics*, **2**(2), P. 6–14 (2011).
- [19] Al'myasheva O. V., Gusarov V. V. Nucleation in media in which nanoparticles of another phase are distributed. *Doklady Physical Chemistry*, **424**(2), P. 43–45 (2009).
- [20] Tugova E. A. GdFeO_3 nanoparticles formation in $\text{Gd}_2\text{O}_3-\text{Fe}_2\text{O}_3-\text{H}_2\text{O}$ system. Proceedings of “Scientific-practical conference dedicated to the 184th anniversary of St. Petersburg state institute of technology foundation”. St. Petersburg, 29-30th of November 2012, P. 200 (2012).